

# Die Geometrical Effect on Annular Die Swelling

YONGSOK SEO\* and EUGENE H. WISLER, *Chemical Engineering Department, University of Texas at Austin, Austin, Texas 78712*

## Synopsis

Die geometrical effect on Newtonian annular jet swelling was studied using a finite element method. Numerical result shows what we expected in the limiting cases of die swelling with annular die geometries, i.e., variation of the die gap for straight dies follows the limiting behavior of capillary and planar die swellings. Also the effect of upstream die geometry was investigated. The result shows that final extrudate dimensions are generally influenced by its previous history in the die, i.e., not only by shearing action but also by elongational effect caused by narrowing die gap.

## INTRODUCTION

Some time ago, a finite element method was used (Seo<sup>1</sup>) for the analysis of the annular die swelling problem, which does not accept any simple reasonable analytical solution due to its complicated geometry originating from two free surfaces, positions of which are not known *a priori*. This article presents a partial result of continuous study of annular die swelling problem.

As is well known, the dimensions of annular jet depend on the swelling ratios, which are influenced by extrusion conditions, rheological properties of polymeric fluids, and die shape. In this article, the effect of die geometry is considered.

According to Allan's computational result,<sup>2</sup> die geometry has a significant effect on the numerical prediction of capillary die swelling. Dealy and his co-workers<sup>3,4</sup> did experimental study about the effect of annular die geometry on final jet swelling ratios. Since they measured relaxed jet swelling instead of instantaneous jet swelling for different shape dies, their result is a little different from the present study. However, their experimental results revealed that extrudate swell is strongly affected by die geometry. Winter and Fischer<sup>5</sup> reported computational result that processing history in annular extrusion dies affects the state of the polymer extrudate at the die exit. Their computational results revealed also that the history of polymer inside the die is influenced by die geometry.

For an annular jet, due to the absence of an axis of symmetry in the fluid, we must consider the entire flow field bounded by the two surfaces of the annular channel. So we can take into considerations of die gap by controlling the radius of inner die wall (represented as dimensionless constant  $k$ ). The

\*To whom all correspondence should be sent.

other study is related to the fact that we can change the fluid history by varying die channel geometry, i.e., by changing its angle (to make a converging or diverging die) and gap width. This makes the fluid experience not only a shearing but also an elongation.

### MATHEMATICAL FORMULATION AND A FINITE ELEMENT SCHEME

The mathematical description of the steady fluid motion is assumed to be given by the following equations:

$$\nabla \cdot \mathbf{v} = 0 \quad (\text{continuity equation}) \quad (1)$$

$$\rho \mathbf{v} \cdot \nabla \mathbf{v} = \rho \mathbf{f} + \text{div } \boldsymbol{\sigma} = -\nabla p + \rho \mathbf{f} + \nabla \cdot \boldsymbol{\tau} \quad (\text{momentum equation}) \quad (2)$$

Here the fluid was assumed to be incompressible and a Newtonian fluid. In these equations,  $\mathbf{v}$  represents the fluid velocity vector,  $\rho$  the density,  $\mathbf{f}$  the body force vector per unit mass,  $\boldsymbol{\tau}$  deviatoric stress tensor,  $\boldsymbol{\sigma}$  total stress tensor ( $= -p\mathbf{I} + \boldsymbol{\tau}$ ), and  $p$  pressure. For the constitutive equation Newtonian fluid was used as mentioned. Then

$$\boldsymbol{\tau} = 2\eta \mathbf{D} \quad (3)$$

where  $\mathbf{D}$  is the rate of strain tensor and  $\eta$  is the Newtonian viscosity. The transport of thermal energy in the fluid is described by

$$\rho C_p \mathbf{v} \cdot \nabla T = S + \nabla \cdot (\mathbf{k} \cdot \nabla T) + \boldsymbol{\tau} : \mathbf{D} \quad (\text{energy equation}) \quad (4)$$

where  $C_p$  is the specific heat,  $S$  is the volumetric heat source,  $\mathbf{k}$  is the thermal conductivity tensor. With the suitable boundary conditions, these four equations form the basis of the finite element method used in this study. Using the variational statement for these equations implicitly included in conjunction with a finite element interpolation for the independent variables  $\mathbf{v}$ ,  $p$ , and  $T$  yields the standard finite element equations. Since the finite element scheme used in this study has been fully described elsewhere,<sup>1</sup> we don't repeat the lengthy and complicated derivation and only mention briefly the main features of this scheme. Basically the finite element method code used here is designed for steady state, incompressible, 2-dimensional (plane or axisymmetric without torsion) fluid problems. It is based on the Galerkin discretization procedure, solving simultaneously eqs. (1)–(4) to their full nonlinear forms. To solve nonlinear terms, iteration was done until convergence occurs using the Newton–Raphson iteration method or the successive substitution method.<sup>1</sup> In this study, we will investigate the annular die swelling of an isothermal Newtonian annular jet extruded from different die geometries, and so the energy equation (4) will not be used. The computer program has been amply tested for correct simulations.

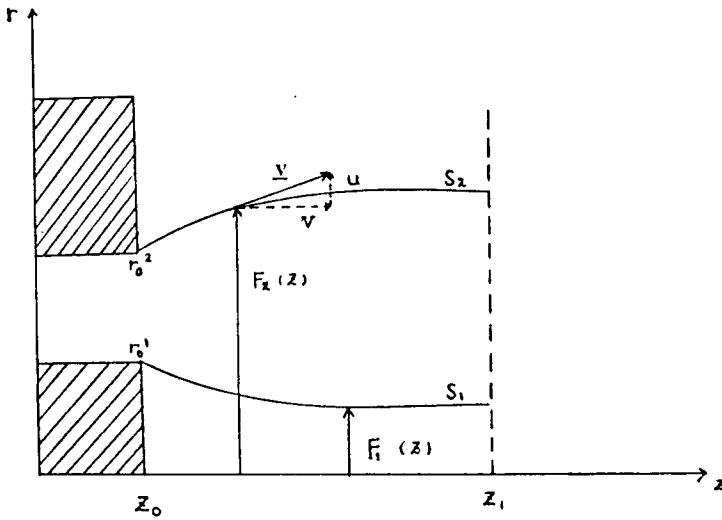


Fig. 1. Description of the free surface problem.

**FREE SURFACE ITERATIONS AND A PROBLEM DESCRIPTION**

In a free surface problem, such as die swelling problem, an additional source of nonlinearity is present since the location of the free surface is not known *a priori*. Consider the fluid emerging from a die into the atmosphere as shown in Figure 1. If the shear stress due to the surrounding air can be ignored, the free surface condition is equivalent to setting the shear stress to zero and the normal stress to the ambient pressure (generally taken as zero). Also in this class of problems, in addition to the nonlinearity due to the unknown free surface location, a singularity is present since the fluid velocity changes from zero (no-slip condition on the wall before emerging from the die) to a non-zero value (the no-shear condition after exiting from the die) in an infinitesimal distance. This is also the situation in what is called a stick-slip problem, except the free surface condition.

The shape of the free surface is calculated by means of an iterative procedure. Let us consider the case of an annular die in Figure 1 with two free surfaces  $S_1$  and  $S_2$  described by the equations

$$r^1 = F_1(z), r^2 = F_2(z), \quad z_0 \leq z \leq z_1 \tag{5}$$

Since the free surface is also a stream surface, we must have

$$\frac{dF_i(z)}{dz} = \frac{u}{v} [z, F_i(z)], \quad F_i(z_0) = r_0^i, \quad i = 1, 2 \tag{6}$$

where  $u$  and  $v$  are the radial and axial velocities, respectively, and  $r_0^i$  are the fixed radius positions at the exit. The iterative procedure starts from cylindrical surfaces on which vanishing contact forces are imposed; new surfaces are

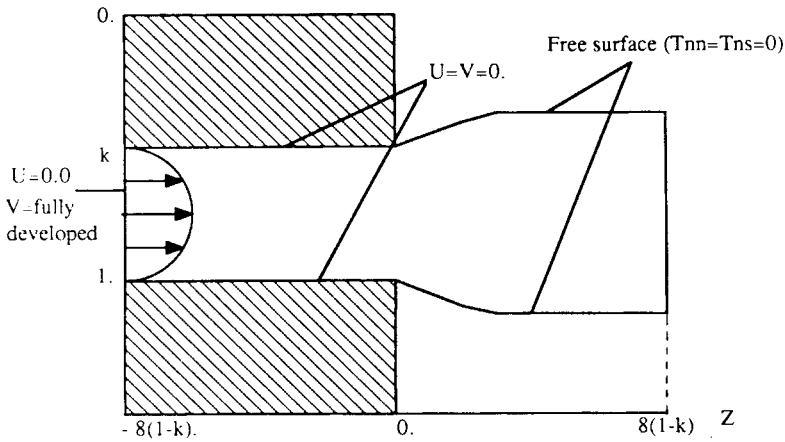


Fig. 2(a). Annular die swelling problem sketch.

defined by the equations

$$\frac{dF_i^{n+1}}{dz}(z) = \frac{u}{v} [z, F_i^n(z)], \quad F_i^{n+1}(z_0) = r_0^i, \quad i = 1, 2 \quad (7)$$

Here  $F_i^n$  means  $n$ th iterated free surfaces. So

$$F_i^{n+1} - F_i^0 (= r_0^i) = \int_{z_0}^{z_1} \frac{u}{v} [z, F_i^n(z)] dz, \quad i = 1, 2 \quad (8)$$

These are integrated by means of Simpson's rule, and generally five or six iterations were enough to produce converged free surface positions, but sometimes it needs more iterations. The problem sketch is shown in Figure 2(a), and its grid is shown in Figure 2(b) for a straight die of  $k = 0.5$ . The upstream and downstream length of the die gap were taken eight times to get converged shapes and exclude die exit disturbances. Through this study, nine node Lagrangian elements were used.

### THE EFFECT OF DIE GAP WIDTH VARIATION

The basic qualitative aspects of the annular jet swelling problem are quite similar to those for the capillary or planar die swelling problems. However, as mentioned before, a major difference is the absence of an axis or plane of symmetry and this necessitates a consideration of the entire flow field bounded by the two surfaces of the annular channel; in another words, we should solve a two-free-surface problem.

The other thing to be mentioned is that for annular jet swelling, we can define three different swelling ratios, inside diameter swelling ( $S_i$ ), outside

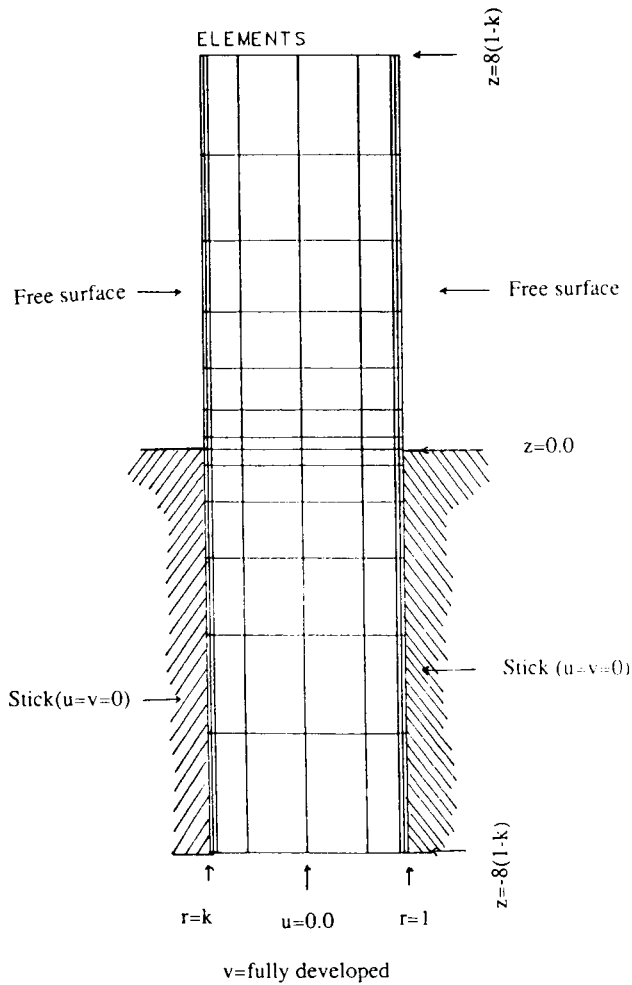


Fig. 2(b). Finite element grid for a die swelling problem.

diameter swelling ( $S_o$ ), and thickness swelling ( $S_t$ ) as follows:

$$S_o = \frac{[R_{out}^{final}(z_\infty) - R_{out}^{initial}(z_\infty)]}{R_{out}^{initial}(z_\infty)} = \frac{R_0^f}{R_0^i} - 1.$$

$$S_i = \frac{[R_{in}^{initial}(z_\infty) - R_{in}^{final}(z_\infty)]}{R_{in}^{initial}(z_\infty)} = 1 - \frac{R_i^f}{R_i^i} \tag{9}$$

$$S_t = \frac{[R_{out}^{final}(z_\infty) - R_{in}^{final}(z_\infty)]}{[R_{out}^{initial}(z_\infty) - R_{in}^{initial}(z_\infty)]} - 1$$

Here  $R_{in}$  means the inside radius,  $R_{out}$  the outside radius,  $z_\infty$  is far down-

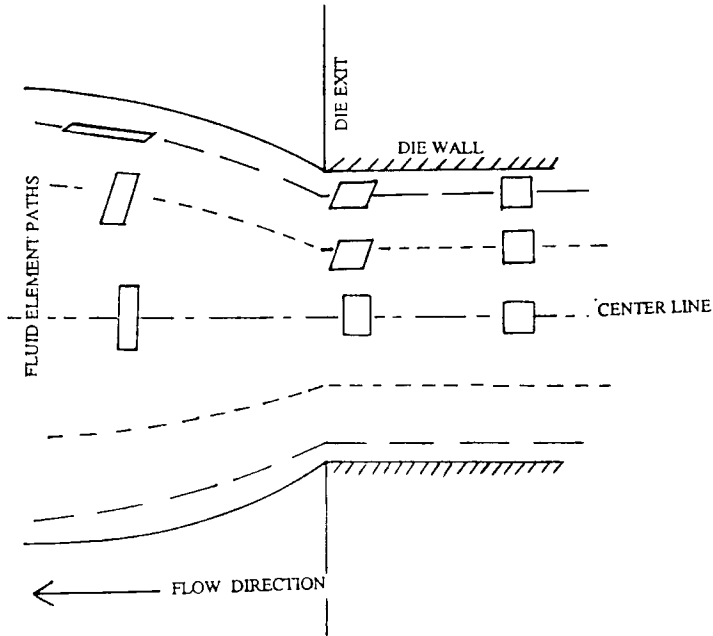


Fig. 3. Fluid element shape changes extruded from straight annular die.

stream, initial means the initial position before free surface iteration, and the final means the final position after free surface iteration. These swelling ratios are related to each other. If  $R_o^i$  and  $R_i^i$  are dimensionless values 1 and  $k$ , respectively, they can be presented as follows:

$$S_o = R_o^f - 1$$

$$S_i = 1 - (R_i^f/k)$$

$$S_i = [R_o^f - R_i^f]/[1 - k] - 1 \quad (10)$$

or

$$S_i = [(1 + S_o) - (1 - S_i)*k]/[1 - k] - 1$$

The dimensionless variables used were  $R_o = 1$ ,  $R_i = k$  ( $= 0.5$ ),  $v_{avg} = 1$ ,  $\rho = 1.E-5$ , and  $\eta = 1$ .

The thickness swelling ratio of an annular jet increases or decreases according to die gap. Following Whipple and Hill's experimental result and analysis for capillary die swelling<sup>6,7</sup> fluid elements (not finite elements) change the shape as sketched in Figure 3. An element, starting as a square at the center line of the channel, decelerates as it passes through the exit region. The once-square element ends up as a rectangle with its short side in the flow direction due to compression. A similar element starting at some position between the center line of the fluid and the wall of the die will be sheared into a parallelogram by the velocity gradient as it is first accelerated and then decelerated to its final swollen shape. During the acceleration and decelera-

TABLE I  
Radial and Axial Total Stress at Die Lips

$k$	Inner lip		Outer lip	
	$\sigma_{rr}$	$\sigma_{zz}$	$\sigma_{rr}$	$\sigma_{zz}$
0.2	-20.34	183.99	-15.94	130.1
0.3	-23.22	191.47	-20	174.78
0.4	-28.41	208.86	-25.5	170.43
0.5	-33.21	215.35	-25	179
0.6	-47.86	270.2	-45.16	239.35
0.7	-55.09	288.02	-53.15	268.59
0.8	-63.21	346.93	-59.98	331.5
0.9	-135.32	588.4	-134.41	573.8

tion, the element shifts away from the center line. The final shape is approximately a parallelogram with the short side aligned parallel to the flow direction. Near the wall, the same starting shape will be accelerated to its final swollen extrudate speed while experiencing a shearing force. During acceleration, the element shifts away from the center line. An element near the wall will have an extended nearly parallelogram final shape with the long side nearly parallel to the flow. (Since the maximum velocity is not exactly at the center line, the deformation of elements near the inner die wall and the outer die wall would be a little bit different from each other, but their shapes would be similar to each other.) The smaller the annular die gap, the larger the shearing action. As a result, deformation of the central element becomes larger, and it pushes other elements near to it. Hence, the radial normal stress at die exit increases with narrowing die gap.

Table I presents radial and axial total stresses at the inner and outer die lips for different dies. Since different meshes were used, these values are not absolutely comparable to each other, but the computational result is consistent with what we expected. Also we can conjecture from this result that the jet thickness swelling would increase as die gap decreases. This can be inferred also from the limiting cases of die gap. Capillary die can be taken as a limiting case when  $k$  goes to zero, and a planar die can be assumed as a limiting case when  $k$  goes to almost 1. By experiments and numerical analysis, it is known that creeping flow for circular flow (flow from capillary die) shows almost 12–13% swelling, and planar extrudate has 19–20% swelling (Tanner<sup>8</sup>). Therefore, it is expected that ideally as  $k$  increases from 0 to 1 the thickness swelling increases from 12–13% to 19–20%, which corresponds to capillary and planar die swellings. Table II summarizes the computational results. This agrees with our expectation. As a reference, Dutta's FDM result<sup>9</sup> is also presented in Table II. However, the FDM scheme failed to work properly for annular dies when the ratio  $k$  lies outside of the range 0.3–0.7. When the ratio  $k$  was less than 0.3, FDM calculations failed to converge, and, for  $k$  larger than 0.7, the results do not appear to be consistent with the expected behavior. With present FEM code, there was not such a problem, which suggests that the difference in annular jet thickness swelling ratios between these two schemes can be attributed to error of FDM results to fit free surface condition. For the planar die swelling problem, Reddy and Tanner<sup>10</sup> got a 20%

TABLE II  
Die Geometry Effect on Annular Jet Swelling (Die Gap Variation)

$k$	$S_i$ (%)	$S_j$ (%)	$S_o$ (%)	FDM <sup>9</sup>
0.2	13.61	-0.3	10.97	—
0.3	13.95	-1.14	10.1	14.86
0.4	14.2	-2.4	9.49	15.59
0.5	14.58	-2.6	8.6	16.47
0.6	15.8	-2.612	7.93	17.14
0.7	16.38	-2.4	6.59	17.48
0.8	17.4	-1.563	4.73	17.51
0.9	18.6	-0.94	2.71	16.48
0.96	19.71	-0.47	1.246	—

thickness expansion, and the result in Table II approaches this value when  $k = 0.96$ . The result in Table II was all for small Reynolds number ( $Re = 1.E - 5$ ).

### THE EFFECT OF UPSTREAM DIE GEOMETRY

Until now, we have considered only a straight annular die. However, annular dies used in polymer processing operations have a flow channel of complex shape with either converging or diverging die walls. Different annular geometries make it possible to generate different flow histories not only of shearing, but also possibly superimposed biaxial extension (by changing the radius and the gap width along the annular channel). This additional deformation affects not only the polymer elements close to die wall, but also the one in the middle of the annulus. For material elements that are subjected to biaxial extension superimposed on shear, it would be necessary to use a different constitutive equation. However, as far as is known, no real constitutive equation can be used to describe such a motion. An arbitrary superposition of shear and biaxial extension in a constitutive equation of integral type was used by Winter and Fischer<sup>5</sup> to study processing histories in extrusion dies, but its applicability is still open to question. Since a Newtonian fluid can be thought of as a limiting case, we would rather use it here.

Two different kinds of die geometries were used as shown in Figure 4. Positive  $\beta$  means a diverging die, and negative  $\beta$  means a converging die. Dies no. 1, 2, and 3 all have the same radius and die gap both far upstream and at the die exit, as do no. 5, 6, and 7. Therefore, their far upstream and die exit geometries are the same, and only the passway (converging and diverging section) lengths and angles are different. The length of converging and diverging sections were 1.637, 0.794, and 0.5 for 10°, 20°, and 30° dies, respectively. Dies no. 4 and 8 has the same far upstream geometry, but their gap size at die exit was reduced using nonparallel walls. Die no. 4 used a 10° converging angle at the inner wall and a 30° converging angle at the outer wall. Die no. 8 used a 30° diverging angle at the inner wall and a 10° diverging angle at the outer wall. The length of the converging and diverging section was taken the same as 30° dies. As before,  $8 \times 13$  meshes were used, and the boundary conditions were the same as for straight-die case [Fig. 2(a)]. The result of these geometries is shown in Table III. In spite of the same extrusion



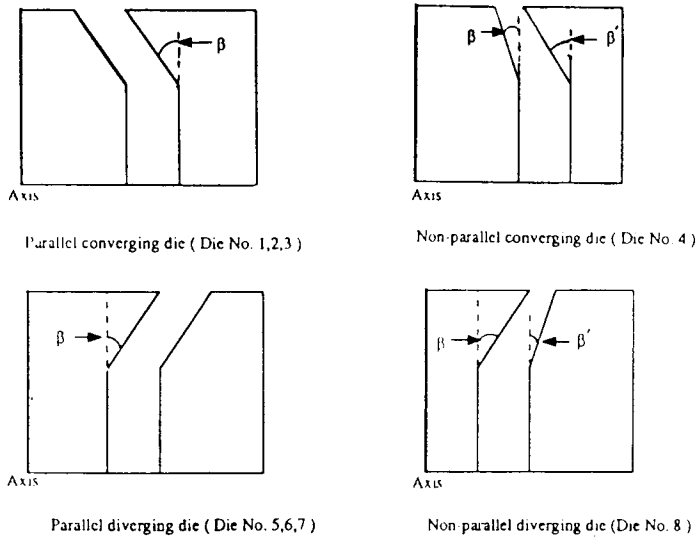


Fig. 4. The geometries of converging and diverging dies.

rate and the same upstream and die exit geometries, the swelling ratios show different behaviors. We can see that converging dies produce reduced outer radius swelling ratios and increased inner thickness swelling ratios compared to those of a straight die. Converging dies no. 1, 2, and 3 have parallel walls, but die no. 4 has a narrowing gap in the direction of flow, so that there is a stretching along stream lines due to decreasing cross section area and a concomitant compression in the hoop direction. According to Winter and Fischer's computational analysis,<sup>5</sup> a tapered section increases the stress ratio of first normal stress difference to shear strain significantly due to the occurrence of extensional flow in converging dies, whereas shear flow reduces the stress ratio to a smaller value for memory fluids. Even though Winter and Fischer's result was not related to die swelling, it seems that a narrowed die would produce more swelling due to large free recovery after injection. For a Newtonian fluid, it can also be expected that the swelling ratios will increase in a die of narrowing gap due to stretching in the flow direction. This is indeed

TABLE III  
Effect of Die Geometry on the Swelling of an Annular Jet,  $k = 0.5$

Die no.	$\beta$ (°)	$S_o$ (%)	$S_i$ (%)	$S_r$ (%)	Remark
1	-30	1.11	32.97	15.51	Converging
2	-20	4.09	23.35	15.69	Converging
3	-10	6.93	12.96	15.22	Converging
4	-10-30	0.72	15.4	19.46	Converging
5	30	36.93	-58.85	2.36	Diverging
6	20	22.77	-33.06	6.54	Diverging
7	10	14.25	-16.15	11.24	Diverging
8	10-30	20.41	-25.51	6.97	Diverging

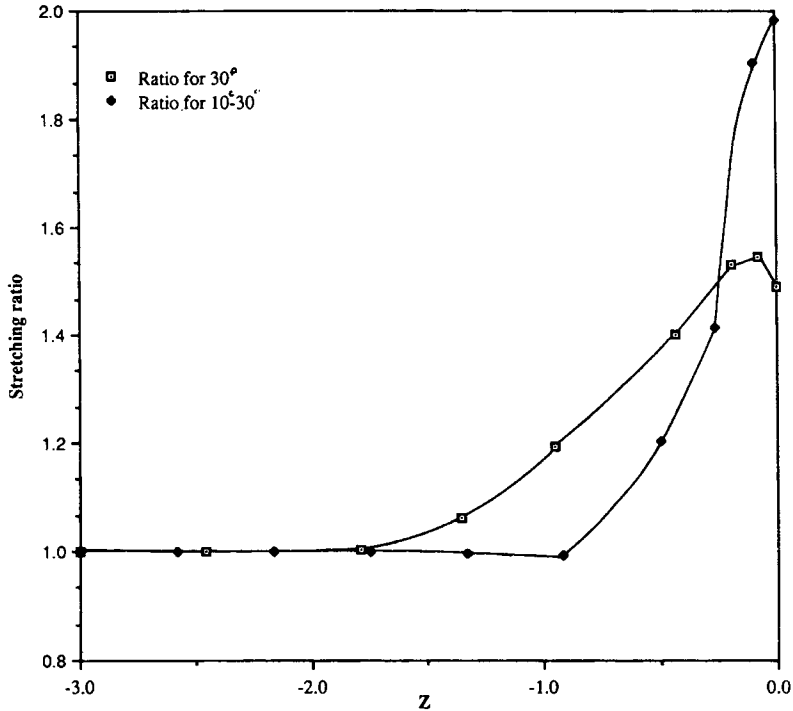


Fig. 5. Axial stretching ratio of the fluid element near the middle of the converging annulus ( $R$  initial = 0.75): ( $\square$ ) ratio for  $30^\circ$ ; ( $\blacklozenge$ ) ratio for  $10^\circ$ - $30^\circ$ .

the case as shown in Table III. The stretching in a flow direction is given by the change of velocity along a streamline.

$$\delta_z(\Psi) = \frac{v'_z(z', \Psi)}{v_z(z, \Psi)} \quad (11)$$

This was calculated for two converging dies and is shown in Figure 5. It agrees with our expectation that a narrowed die has a larger stretching.

For diverging dies, we have a circumferential or hoop stretching of the melt and a concomitant deceleration along the streamlines. This will decrease the thickness swelling ratio due to decreased shearing action. Table III reveals that the thickness swelling ratio is reduced with increasing diverging angle (no. 5, 6, and 7). For die no. 8 with nonparallel walls ( $10^\circ$  and  $30^\circ$  diverging angles for outer and inner walls, respectively), the stretching in the flow direction prevents hoop stretching, and we can expect that the thickness swelling ratio of die no. 8 would be smaller than for the  $10^\circ$  diverging die but larger than for the  $30^\circ$  diverging die. This is indeed the case, as in Table III. Like axial stretching, the stretching in circumferential direction corresponds to a change of radial position of the streamline:

$$\delta_r(\Psi) = \frac{r'_z(z', \Psi)}{r_z(z, \Psi)} \quad (12)$$

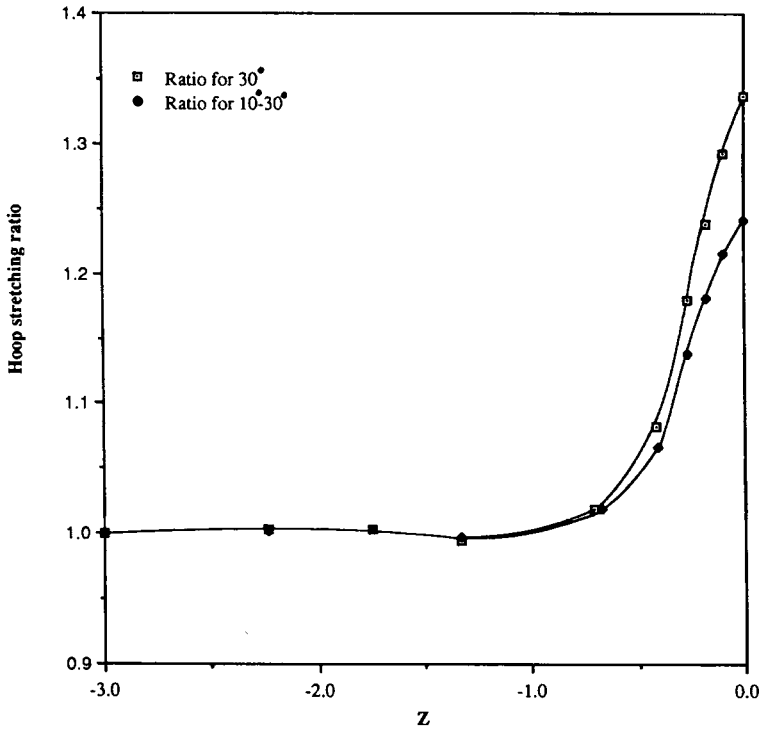


Fig. 6. Hoop stretching ratio of the fluid element near the middle of diverging annulus ( $R$  initial = 0.736): ( $\square$ ) ratio for  $30^\circ$ ; ( $\blacklozenge$ ) ratio for  $10^\circ-30^\circ$ .

This was calculated for two diverging dies ( $30^\circ$  diverging die and  $10^\circ-30^\circ$  diverging die). The result is shown in Figure 6. It can be seen clearly that the narrowed die has smaller stretching in radial direction than a die with parallel walls due to counteracting axial direction stretching.

From Table III we can also see different annular jet movements. Cogswell and Lamb<sup>11</sup> derived the following approximate relationship for annular die swelling based on a number of simplifying assumptions:

$$S_t = S_o^2 \quad (13)$$

Henze and Wu<sup>12</sup> found from their studies of parison swelling that

$$S_t = S_o^3 \quad (14)$$

However, no simple relationship between  $S_t$  and  $S_o$  is apparent in Table III. Orbey and Dealy<sup>3</sup> concluded that the relative magnitudes of the thickness and diameter swellings can be independently controlled by appropriate die design features. The computational results also support this opinion. Another fact that attracts attention is that when  $k$  is close to 1, it is possible to use a Cartesian coordinate system instead of a cylindrical coordinate system, but, for converging or diverging die case, this would not be a good approximation since in a Cartesian coordinate system, because of no hoop stress, the fluid

does not have a converged shape but keeps moving in the flowing direction for the converging or the diverging die case. When the same calculation was done for the annular jet coming out of a  $30^\circ$  diverging die of  $k = 0.96$ , the Cartesian coordinate system calculation shows 24.58% thickness swelling ratio at far downstream (its inner and outer surfaces did not have converged shapes), while the cylindrical coordinate system calculation shows 18.38% thickness swelling at far downstream. As expected, use of a cylindrical coordinate system gives less thickness swelling ratio due to hoop stress. That is because in a Cartesian coordinate system the hoop stress is zero, but in a cylindrical coordinate system this value is not zero.

### CONCLUSION

The result of this work shows that not only shearing but also elongational effect plays an important role in annular die swelling phenomena. Also, die gap variation affects annular die swelling ratios due to different shearing action. From the computational result, a simple relationship between the ratios of thickness swelling and outer radius swelling could not be found. Even though this study was limited to a Newtonian fluid case, it reveals that die geometry affects strongly the final extrudate dimensions. For a viscoelastic fluid case, the problem will be more complicated. This direction in research is under investigation and will be reported on in the future.

### References

1. Y. Seo, Ph.D. dissertation, University of Texas at Austin, 1987.
2. W. Allan, *Int. J. Numer. Methods Eng.*, **11**, 1621 (1977).
3. N. Orbey and J. M. Dealy, *Polym. Eng. Sci.*, **24**(7), 511 (1984).
4. A. Garcia and J. M. Dealy, *Polym. Eng. Sci.*, **22**(3), 158 (1982).
5. H. H. Winter and E. Fischer, *Polym. Eng. Sci.*, **21**(6), 266 (1981).
6. B. A. Whipple and C. T. Hill, *AIChE J.*, **24**, 664 (1978).
7. B. A. Whipple, Ph.D. dissertation, Washington University, St. Louis, 1974.
8. R. I. Tanner, in *Computational Analysis of Polymer Processing*, J. R. A. Pearson, Ed., Applied Science, London, 1983.
9. A. Dutta, Ph.D. thesis, State University of New York, Buffalo, 1981.
10. K. R. Reddy, and R. I. Tanner, *J. Rheol.* **22**, 661 (1978).
11. F. N. Cogswell and P. Lamb, *Plast. Polym.*, **38**, 331 (1970).
12. E. D. Henze and W. C. L. Wu, *Polym. Eng. Sci.*, **13**, 153 (1973).

Received October 1, 1987

Accepted January 21, 1988